

## Consolidation of amorphous $\text{Al}_{86}\text{Ni}_6\text{Co}_2\text{Gd}_6$ melt-spun ribbons by twist extrusion

V.N. Varyukhin<sup>1</sup>, V.I. Tkatch<sup>1,a</sup>, V.V. Maslov<sup>2</sup>, Y. Y. Beygelzimer<sup>1</sup>, S.G. Synkov<sup>1</sup>, V.K. Nosenko<sup>2</sup>, S.G. Rassolov<sup>1</sup>, A.S. Synkov<sup>1</sup>, V.I. Krysov<sup>1</sup>,  
V.A. Mashira<sup>2</sup>

<sup>1</sup>Donetsk Institute of Physics & Engineering of the NAS of Ukraine, 72 R. Luxemburg St., Donetsk, 83114, Ukraine.

<sup>2</sup>Institute for Metal Physics of the NAS of Ukraine, 36 Vernadsky St., Kyiv, 03142, Ukraine

<sup>a</sup>vit@depm.fti.ac.donetsk.ua

**Keywords:** nanostructured materials, twist extrusion, amorphous melt-spun ribbons, consolidation, microhardness.

### Abstract.

Amorphous  $\text{Al}_{86}\text{Ni}_6\text{Co}_2\text{Gd}_6$  ribbons produced by melt-spinning processing were consolidated using twist extrusion (TE). Electrical resistance measurements showed that under continuous heating at 5 K/min crystallization begins at 473 K by formation of Al-nanocrystals and ends at 673 K by formation of equilibrium intermetallics. From one to five TE extrusion passes were conducted in several experiments at temperatures 458-573 K and applied pressures ranged between 1150-1700 MPa. The fully dense billets with dimensions  $14 \times 23 \times 40 \text{ mm}^3$  were produced at extrusion temperatures  $\geq 523 \text{ K}$ . The maximum microhardness ( $550 \text{ kgf/mm}^2$ ) was reached for the bulk materials consolidated at 523 K with a nanocomposite structure consisted of Al-nanocrystals with size about 13 nm embedded in amorphous matrix. The billet compacted at 573 K has a fully crystallized structure and lower microhardness ( $380 \text{ kgf/mm}^2$ ).

### Introduction

Nanostructured materials (NSM) have attracted the growing interest due to their unique physical and technologically important properties owing to the extremely small grain dimensions [1]. There are two main approaches to synthesize materials with ultra fine-grained structures. The one way involves the use of severe plastic deformation (SPD) methods providing very large strains at relatively low temperatures [2,3]. Another way of producing NSM is based on non-equilibrium crystallization from liquid or amorphous states [4,5] which allows producing unique structural states with improved both strength and ductility. In part, in Al-based Al-TM-RE alloys (TM are transition and RE are rare earth metals) with partially crystallized nanocomposite structure (Al-nanocrystals embedded in amorphous matrix) ultimately high strength of about 1500 MPa was achieved [5]. In this case, NSM is produced by two step process including (1) formation of amorphous phase by rapid cooling of liquid alloy and (2) subsequent controlled crystallization of glassy alloy under heat treatment.

However, amorphization of Al-based alloys requires high cooling rates (typically above  $10^5 \text{ K/s}$ ) and glassy materials can be obtained only in ribbon, flake or powder forms with a maximum size less than  $100 \mu\text{m}$  at least in one dimension. Therefore, consolidation of the rapidly cooled products is required to fabricate bulk high-strength nanostructured materials usable for industrial applications. It should be noted that using of conventional hot extrusion or hot pressing techniques for full consolidation of Al-based powder requires rather high temperatures ( $\geq 673 \text{ K}$ )

[4,6] at which phase transformations and excessive structural coarsening processes occur influencing in a detrimental way the alloy properties.

On the other hand, investigations showed that SPD methods can be used successfully not only for the refinement of a microstructure but also for the low-temperature consolidation of powders [2,7] and these results stimulated experiments on compaction of rapidly materials with non-equilibrium structures. In part, it has been recently established that severe plastic torsion straining at ambient temperature allows to obtain NSM materials by compacting of semi-amorphous Al-based powders prepared by mechanical alloying and gas atomization processing [8] as well as of amorphous  $\text{Ti}_{50}\text{Ni}_{25}\text{Cu}_{25}$  and  $\text{Fe}_{82.3}\text{Ni}_{11.8}\text{B}_{5.9}$  alloys ribbons produced by melt spinning technique [9]. The fully consolidated disk-shape samples 0.2-0.3 mm thick have improved physical properties, but, however, the high-pressure torsion straining process does not allow to produce large bulk materials.

Equal channel angular extrusion (ECAE) is another SPD technique which has been used for consolidation of partially amorphous Al-TM-RE alloy gas-atomized powder at 280 °C [10], but full density of compacted samples was not achieved, probably owing to presence of high volume fraction of brittle intermetallic phase [11]. In view of technological interest to further examine the possibility of obtaining fully dense NSM materials from amorphous precursors in the present study the twist extrusion (TE) processing was used for the first time for consolidation of amorphous  $\text{Al}_{86}\text{Ni}_6\text{Co}_2\text{Gd}_6$  melt-spun ribbons.

Twist extrusion (TE) is a relatively new method of SPD [12]. In this technique, a billet material is subjected to severe shear deformation by forcing it around an axis during pushing through the die with the twisted channel (Fig. 1). As a result of extrusion pass the cross section area of samples remains unchanged and their repeat deformation is possible.

## Experimental Procedure

The ingot of  $\text{Al}_{86}\text{Ni}_6\text{Co}_2\text{Gd}_6$  alloy (atomic percent) was prepared by induction melting of the preliminary prepared  $\text{Al}_3\text{Gd}$  compound and Al (99.99%), Ni and Co ( $\geq 99.9\%$ ) under purified argon. The rapidly quenched ribbons were produced by planar flow casting of melt onto a rotating copper wheel using a quartz nozzle in atmosphere of pure helium. The wheel surface speed was 25 m/s, the ejection overpressure was  $\geq 25$  kPa, the melt temperature was 1223 K and the nozzle-wheel was gap 0.2 mm. The resultant fully ductile ribbons had a width of 15 mm and thickness of 40-60  $\mu\text{m}$ . The chemical compositions of the master alloy and melt-spun ribbons were checked by the X-ray fluorescence analysis.

For TE consolidation the melt-spun ribbons without preliminary milling were placed into copper cans of 30 mm outer diameter and 100 mm height and cold compacted to about 73% theoretical density and then the cans were sealed. In this experiments the die having a twist channel with a rectangular cross-section  $15 \times 25 \text{ mm}^2$  and a twist line angle  $\beta$  of  $60^\circ$  was used (Fig. 1). Prior extrusion the die and a can were preheated to the selected temperature during about 15 min and then extruded at the rate 3 mm/s with anti-pressure applied to calibrating part of the channel. As it has been shown [13] the accumulated deformation in every extrusion pass is about 1.15. During first extrusion pass the can with compacted ribbon changed a shape of its cross section which remained unchanged during subsequent passes. From one to five extrusion passes were conducted in several experiments at temperatures 458-573 K and applied pressures ranged between 1150-1700 MPa and the billets with dimensions of  $15 \times 25 \times 40 \text{ mm}^3$  were produced.

X-ray diffraction was used to characterize the structure of the as-prepared and heat treated ribbons as well as the compacted billets using a DRON-3M diffractometer with Fe-filtered  $\text{CoK}_\alpha$  radiation. The microstructure of consolidated samples was investigated by light microscopy using Neophot-32 microscope. Microhardness of the melt-spun ribbons and consolidates was measured using a standard PMT-3 microhardness tester under a load of 0.29 N (30 gf) applied for 10 s. The data presented are the average value of 10 indentations and the standard deviation of data does not exceed 2%.

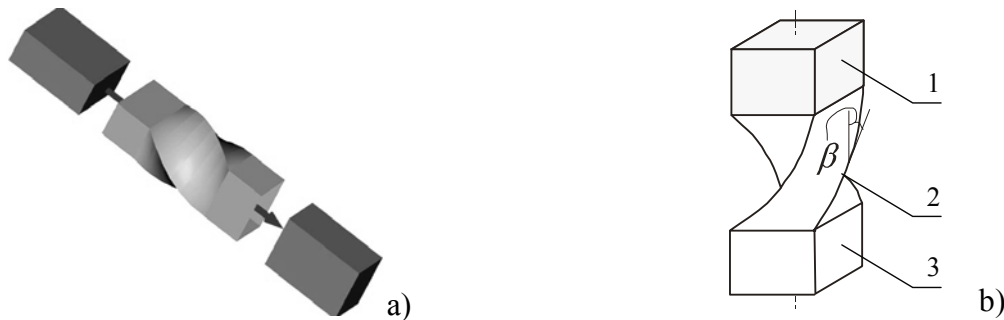


Fig. 1. Schematic illustration showing the principle of TE processing: (a) passing a sample through the channel and (b) the shape of the twist channel with the input (1), twist (2) and calibrating (3) parts and the twist line angle  $\beta$ .

The thermal stability of the as-prepared ribbons was studied by electrical resistance measurements by a four-probe dc technique at heating rate of 5 K/min. The density of the bulk samples were measured using the Archimedes method.

## Results and Discussion

The X-ray diffraction studies showed that the as-quenched melt-spun  $\text{Al}_{86}\text{Ni}_6\text{Co}_2\text{Gd}_6$  ribbons were fully amorphous (Fig. 2a). Within a wide  $2\theta$  range ( $30\text{-}60^\circ$ ) only a dispersive peak was seen, without any trace of sharp peaks related to periodic lattice structure. The microhardness ( $H_\mu$ ) of the ribbons with amorphous structure was measured to be  $360 \text{ kgf/mm}^2$  (Table 1) which is somewhat higher than of the Al-Ni-Y glasses [14] with the same content of solutes.

In order to estimate the temperatures regimes of consolidation the behaviour of the melt-spun ribbons under continuous heating has been preliminary studied. It has been established from the electrical resistance measurements that crystallization of amorphous  $\text{Al}_{86}\text{Ni}_6\text{Co}_2\text{Gd}_6$  ribbons under constant rate heating occurs via three clearly separated stages. The onset crystallization temperature at heating rate 5 K/min was found to 473 K while all transformation was completed at approximately 573 K. The X-ray studies of the ribbons heated up to different temperatures have shown that the first transformation stage of the amorphous phase is primary crystallization which results in formation of nanocomposite structure (Al particles + remaining amorphous phase). During the second crystallization stage fine metastable unidentified phases formed while structure of the fully crystallized specimens consisted of relatively coarse crystals of Al and equilibrium intermetallic compounds ( $\text{Al}_3\text{Gd}$ ,  $\text{Al}_3\text{Ni}$ ,  $\text{Al}_9\text{Co}_2$ ). Temperatures of the crystallization stages completion are listed in Table 1.

Table 1  
Temperatures of the end of the crystallization stages of amorphous  $\text{Al}_{86}\text{Ni}_6\text{Co}_2\text{Gd}_6$  ribbons at heating rate of 5 K/min and the corresponding values of microhardness and volume crystallized

$T, \text{K}$	293	593	620	673
$H_\mu, \text{kgf/mm}^2$	$360 \pm 5$	$552 \pm 7$	$620 \pm 10$	$468 \pm 8$
$X$	0	$0.26 \pm 0.03$	$0.33 \pm 0.04$	1

Crystallization of amorphous phase changes the microhardness of the ribbons. As is seen from Table 1 appearance of the nanocrystalline phases in the amorphous matrix at the first and second crystallization stages results in essential hardening of the nanocomposite structures while formation of relatively coarse crystals at the final stage lowers the microhardness.

In accordance with data on thermal stability of amorphous structure the melt-spun ribbons have been attempted to consolidate with the use of TE at 458 K which is about 20 K lower than the

onset crystallization temperature. It has been established that this extrusion regime is not sufficient to consolidate the ribbons and only processes of milling of the initially long pieces of the ribbons into particles with several mm size occur. Nevertheless, the X-ray analysis of the grinded material showed the presence of a small amount of crystalline phase (fcc Al-nanocrystals). It implies that the severe plastic deformation facilitates crystallization process. This is in general accordance with the results of Ref. [9] where formation of nanocrystalline phase was observed during plastic torsion straining of amorphous  $\text{Ti}_{50}\text{Ni}_{25}\text{Cu}_{25}$  ribbons at room temperature.

The experiments performed at higher TE extrusion temperatures showed that partial consolidation of the amorphous ribbons takes place at temperatures 493-513 K while the fully dense billets have been obtained TE extrusion at temperatures  $\geq 523$  K. Fig. 3 shows the microstructure of the etched sample consolidated via three TE extrusion passes at 523 K. The voids and cracks have not detected in the structure while the separate ribbons without any structural features at the boundaries may be identified.

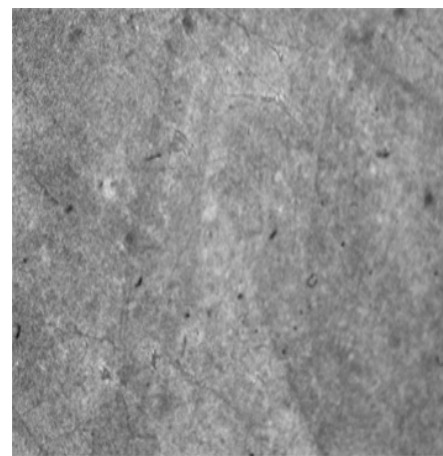
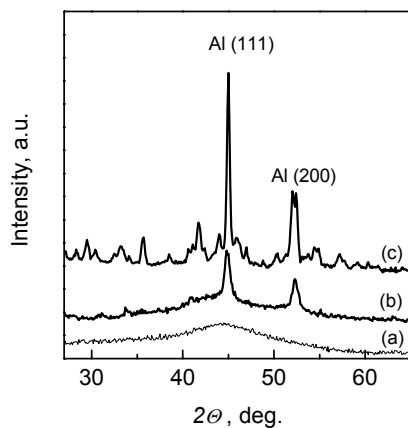


Fig. 2. X-ray diffraction patterns of the as-cast melt-spun  $\text{Al}_{86}\text{Ni}_6\text{Co}_2\text{Gd}_6$  ribbon (a) and the samples consolidated by TE at 523 K (3 passes) (b) and at 573 K (c).

Fig. 3. Optical micrograph of the five-pass TE ribbons compacted at 513 K.  $\times 1000$

The measurements of microhardness of the consolidated samples showed that with increasing of extrusion temperature  $H_\mu$  increased, exhibited a maximum at temperature 513 K, and then decreased (fig. 4). It should be noted that the maximum value of microhardness of consolidated samples ( $550 \text{ kgf/mm}^2$ ) is essentially higher than  $H_\mu$  of the as-prepared amorphous ribbons, but lower than the maximum value achieved in the partially crystallized ribbons (Table 1). It means that the regimes of TE extrusion processing (both extrusion temperature and number of passes) of the melt-spun ribbons may be optimized to enhance the microhardness of the compacted billets. Nevertheless, the microhardness achieved in the TE extruded  $\text{Al}_{86}\text{Ni}_6\text{Co}_2\text{Gd}_6$  samples is higher than the hardness of the material obtained by ECAE processing of the semi-amorphous  $\text{Al}_{85}\text{Ni}_{10}\text{Y}_{2.5}\text{La}_{2.5}$  alloy powder [10].

From comparison between the results of the  $H_\mu$  measurements and the X-ray studies of structure of the consolidated samples (Fig. 2) it follows that the maximum hardness was reached for the bulk materials with partially crystallized structure. As seen in Fig. 2b the X-ray diffraction of the sample consolidated at 523 K show co-existence of a fcc crystalline phase (Al) and a residual amorphous phase. The (111) and (200) peaks of Al are broad enough to use the Scherrer equation  $D = 0.9\lambda/(B \cos\theta)$  (where  $B$  is the full width of the peak at half maximum and  $\theta$  is the Bragg angle) to

estimate the mean grain size  $D$ . The estimations of  $B$  were made by deconvoluting of the total profile of the amorphous halo and the peaks of Al phase as it has been done in Ref. [15].

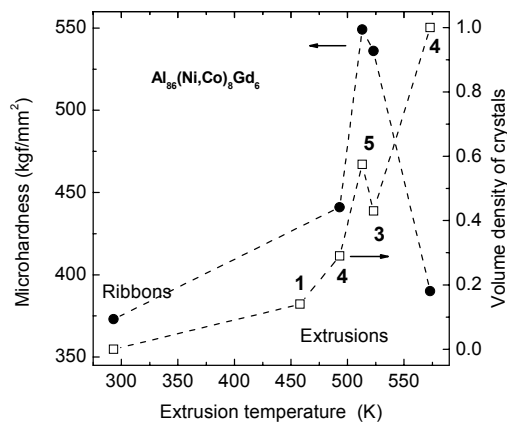


Fig. 4. Microhardness of the amorphous ribbons before and after consolidation (left axis) and the volume fraction crystallized in the compacted samples (right axis) as function of the extrusion temperature. Numbers represent the number of TE passes.

Besides, the halo deconvolution procedure allows to evaluate the crystallized volume fraction  $X$  in partially crystallized samples. The sizes of Al-nanocrystals in samples consolidated at 513-523 K estimated from the X-ray analysis data are  $13 \pm 1$  nm while the volume fraction of nanocrystalline phase is ranged between 0.4-0.5. The sample consolidated at 573 K has fully crystallized structure which contains the same phases as the above mentioned ribbon specimens. Note that the fully crystallized bulk sample has lower microhardness ( $380 \text{ kgf/mm}^2$ ) compared with those of the samples with the nanocomposite structure, but it is still somewhat higher than  $H_{\mu}$  of the amorphous ribbons. From the data presented in Figures 2 and 4 follows that formation of the nanoscale Al crystals in amorphous matrix during consolidation leads to hardening of the materials while formation of the equilibrium intermetallics in the residual amorphous matrix as well as coarsening of the Al phase (Fig. 3c) lowers the hardness. It is also evident from the data

presented in Fig. 4 the volume fraction of nanocrystalline phases in the consolidated samples depends not only on the extrusion temperature but also on number of extrusion passes. It indicates that the structure and consequently mechanical properties of the materials consolidated by TE may be controlled at least by two processing parameters. It is also expected that further studies which are in progress now will allow to develop new high-strength nanostructured Al-based alloys available for practical exploitation.

## Conclusions

Consolidation of amorphous  $\text{Al}_{85}\text{Ni}_6\text{Co}_2\text{Gd}_6$  melt-spun ribbons by severe plastic deformation using the twist extrusion technique was carried out at temperatures 458-575 K and applied pressures of 1150-1700 MPa. Comparison of structural changes in the annealed melt-spun ribbons and those in the compacted samples shows that severe plastic deformation induced by twist extrusion facilitates crystallization process. Fully dense billets with dimensions of  $15 \times 25 \times 40 \text{ mm}^3$  were obtained at temperatures  $\geq 523$  K while partial consolidation of the amorphous ribbons occurred at temperatures 493-513 K. The maximum microhardness as high as  $550 \text{ kgf/mm}^2$  was achieved for the bulk materials consolidated at 523 K with a nanocomposite structure consisted of Al-nanocrystals with size about 13 nm embedded in amorphous matrix. The billet compacted at 573 K has a fully crystallized structure and lower microhardness ( $380 \text{ kgf/mm}^2$ ). The studies performed indicate the potential of TE processing for producing high-strength bulk Al-based alloys with nanocomposite structure from amorphous precursors.

**References**

- [1] H. Gleiter: *Acta Mater.* Vol. 48 (2002), p. 1.
- [2] R.Z. Valiev, R.K. Islamgaliev, I.V. Alexandrov: *Progr. Mater. Sci.* Vol. 45 (2000), p. 103.
- [3] Y.T. Zhu, T.C. Lowe, T.G. Langdon: *Scr. Mater.* Vol. 51 (2004), p. 825.
- [4] A. Inoue: *Progr. Mater. Sci.* Vol. 43 (1998), p. 365.
- [5] A. Inoue, H. Kimura: *Mater. Sci. Eng. A* Vol. 286 (2000), p. 1.
- [6] I. Todd, Z. Chlup, J.S. O'Dwyer, M. Lieblich, A. Garcia-Escorial: *Mater. Sci. Eng. A* Vol. 375-377 (2004)p. 1235.
- [7] K. Matsuki, T. Aida, T. Takuchi, J. Kusui, K. Yokoi: *Acta Mater.* Vol. 48 (2000), p. 2625.
- [8] W.J. Botta Filho, J.B. Fogagnolo, C.A.D. Rorigues, C.S. Kiminami, C. Bolfarini, A.R. Yavari: *Mater. Sci. Eng. A* Vol. 375-377 (2004), p. 936.
- [9] R.Z. Valiev, V.G. Pushin, D.V. Gunderov, A.G. Popov: *Dokl. Akad. Nauk* Vol. 398 (2004), p. 54.
- [10] O.N. Senkov, D.B. Miracle, J.M. Scott, S.V. Senkova: *J. Alloys and Compounds* Vol. 365 (2004), p. 126.
- [11] O.N. Senkov, S.V. Senkova, J.M. Scott, D.B. Miracle: *Mater. Sci. Eng. A* Vol. 393 (2005), p. 12.
- [12] Y. Beygelzimer, D. Orlov, V. Varyukhin: *Ultrafine Grained Materials II* (The Minerals, Metals & Materials Society, Warrendale 2002), p. 297.
- [13] Y. Beygelzimer, V. Varyukhin, D. Orlov, B. Efros, V. Stolyarov, H. Salimgareyev: *Ultrafine Grained Materials II* (The Minerals, Metals & Materials Society, Warrendale 2002), p. 43.
- [14] H.S. Kim: *Mater. Sci. Eng. A* Vol. 304-306 (2001), p. 327.
- [15] W.J. Botta, D. Negri, A.R. Yavari: *J. Non-Cryst. Solids* Vol. 247 (1999), p. 19.